ARL-TR-8631 • JAN 2019

US Army Research Laboratory

Consistent Electrostatics of Crystalline Conductors: Spherical Geometry

by Steven B Segletes

NOTICES

Disclaimers

The findings in this report are not to be construed as an official Department of the Army position unless so designated by other authorized documents.

Citation of manufacturer's or trade names does not constitute an official endorsement or approval of the use thereof.

Destroy this report when it is no longer needed. Do not return it to the originator.

ARL-TR-8631 • JAN 2019

US Army Research Laboratory

Consistent Electrostatics of Crystalline Conductors: Spherical Geometry

by Steven B Segletes
Weapons and Materials Research Directorate, ARL

REPORT DOCUMENTATION PAGE

Form Approved
OMB No. 0704-0188

PLEASE DO NOT RETURN YOUR FORM TO THE ABOVE ADDRESS.

1. REPORT DATE *(DD-MM-YYYY)*	2. REPORT TYPE	3. DATES COVERED (From - To)
January 2019	Technical Report	SEPTEMBER 2018–NOVEMBER 2018

4. TITLE AND SUBTITLE
Consistent Electrostatics of Crystalline Conductors: Spherical Geometry

5a. CONTRACT NUMBER

5b. GRANT NUMBER

5c. PROGRAM ELEMENT NUMBER

6. AUTHOR(S)
Steven B Segletes

5d. PROJECT NUMBER

5e. TASK NUMBER

5f. WORK UNIT NUMBER

7. PERFORMING ORGANIZATION NAME(S) AND ADDRESS(ES)
US Army Research Laboratory
ATTN: RDRL-WMP-C
Aberdeen Proving Ground, MD 21005-5066

8. PERFORMING ORGANIZATION REPORT NUMBER
ARL-TR-8631

9. SPONSORING/MONITORING AGENCY NAME(S) AND ADDRESS(ES)

10. SPONSOR/MONITOR'S ACRONYM(S)

11. SPONSOR/MONITOR'S REPORT NUMBER(S)

12. DISTRIBUTION/AVAILABILITY STATEMENT
Approved for public release; distribution is unlimited.

13. SUPPLEMENTARY NOTES
author's email: <steven.b.segletes.civ@mail.mil>.

14. ABSTRACT
This report extends prior work in the electrostatics of crystalline conductors by developing results for problems possessing a spherical geometry. While still a 1-D result, the work offers new insights that cannot be made for 1-D Cartesian (and/or cylindrical) geometries, in that only the spherical geometry analyzes a body of finite dimensions. Thus, results in the far field can be studied to see if they match expectations gleaned from classical electrostatics. Inside the body, however, the volumetric charge density of positive charges is limited to a finite value, unlike mobile negative charges, which can congregate on a body's periphery with an infinite volumetric density (by way of a finite surface-charge density). It is this asymmetry between allowable positive/negative charge densities that leads to results that are at odds with classical electrostatic theory.

15. SUBJECT TERMS
electrostatic potential, charge distribution, surface density, Poisson equation, spherical geometry

16. SECURITY CLASSIFICATION OF:			17. LIMITATION OF ABSTRACT	18. NUMBER OF PAGES	19a. NAME OF RESPONSIBLE PERSON
a. REPORT	b. ABSTRACT	c. THIS PAGE			Steven B Segletes
Unclassified	Unclassified	Unclassified	UU	39	19b. TELEPHONE NUMBER (Include area code) 410-278-6010

Contents

List of Figures v

List of Tables vi

Acknowledgments vii

1. Introduction 1

2. Governing Equations 3

2.1 Poisson Equation for a Spherical Geometry 4

2.2 Domain-Interface Continuity/Jump Conditions 5

2.3 Total Quantity of Charges 6

3. 1-D Solutions for a Spherical Geometry 7

3.1 Configuration 1 7

3.1.1 Charge Tally 7

3.1.2 Electrostatic Potential and Electric Field 8

3.1.3 Configuration 1: Final Result 10

3.2 Configuration 2 10

3.2.1 Charge Tally 10

3.2.2 Electrostatic Potential and Electric Field 12

3.2.3 Configuration 2: Final Result 15

3.3 Configuration 3 17

3.3.1 Charge Tally 17

3.3.2 Electrostatic Potential and Electric Field 18

3.4 Configuration 3a 18

3.5 Configuration 3b 20

3.5.1 Charge Tally 21

3.5.2 Electrostatic Potential and Electric Field 22

3.5.3 Configuration 3b: Final Result 24

4. Conclusion 26

5. References **28**

Distribution List **29**

List of Figures

Fig. 1 Cross-sectional (cutaway) geometry of a conductor 2

Fig. 2 Configuration 1, comprised solely of a neutral Ω_n domain (gray), with mobile negative charges concentrated at the external S_n boundary 8

Fig. 3 Configuration 1 potential $\varphi(r)$, for the case where $Q_{\text{net}} = -R_s^2$ 11

Fig. 4 Configuration 2, with finite Ω_a domain (red) at the external boundary .. 12

Fig. 5 Configuration 2 potential $\varphi(r)$, for the case where $Q_{\text{net}} = R_s^2$ 16

Fig. 6 Configuration 3, with finite Ω_a domain (red) at the sphere center boundary 17

Fig. 7 Configuration 3a, with Ω_a domain (red) sandwiched between two neutral Ω_n domains 20

Fig. 8 Configuration 3b, with internal void between Ω_a domain (red) and an infinitesimally thin S_n interface 21

Fig. 9 Configuration 3b potential $\varphi(r)$, for three cases spanning $Q_{\text{net}} > 0$, $Q_{\text{net}} = 0$, and $Q_{\text{net}} < 0$ 25

List of Tables

Table 1 Domain constraints on Eq. 2 5
Table 2 Configuration 1: equations by domain 9
Table 3 Configuration 1: unknowns and interface continuity/jump equations 9
Table 4 Configuration 2: equations by domain 13
Table 5 Configuration 2: unknowns and interface continuity/jump equations ... 13
Table 6 Configuration 3: equations by domain 19
Table 7 Configuration 3: unknowns and interface continuity/jump equations ... 19
Table 8 Configuration 3b: equations by domain 23
Table 9 Configuration 3b: unknowns and interface continuity/jump equations . 23

Acknowledgments

I would like to express my sincere gratitude to Dr M Grinfeld for the productive collaborations in which we have engaged over the years. I thank him for his encouragement to write this report as a sequel to our recent collaboration. During this effort, he stood ready to provide advice and clarification that enhanced the quality and focus of this effort. His review of the work helped immeasurably.

I am, again, extremely grateful for the efforts of Ms Carol Johnson, my longtime editor, for the excellent job she does in improving the content of my reports.

1. Introduction

The computational modeling of fields involving discontinuities can pose many challenges to convergence. Strategies to overcome these challenges may be based on the actual physics or purely on the numerics, but often involve smearing out the discontinuity that exists in the physical space, to avoid sharp gradients from manifesting in a discretized domain. One example of this is artificial viscosity, which is used to reduce the steepness of gradients across a shock discontinuity, in the hope of promoting numerical convergence.

In the field of computational magnetohydrodynamics (MHD), a comparable discontinuity is encountered in the form of electric charge density. According to classical electrostatics theory, which is intrinsic to many computational-MHD formulations, excess electric charge (either positive or negative) in a body will, to attain equilibrium, build up in an infinitesimally thin layer on the surface of the body.

For crystalline materials (as an example), positive ions are not mobile (*i.e.*, they are *not* free to congregate on an infinitesimally thin body-surface layer). Rather, they are nailed to the lattice geometry in a way that limits their maximum volumetric density. Adapting the classical approach in a way to limit the maximum volumetric density of positive charge not only has relevance to this aspect of the physics, but can have the ancillary benefit of removing the field discontinuity (insofar as excess positive charge) that can otherwise challenge the convergence of an associated discretization.*

In prior reports[1,2] on the subject, Grinfeld and Segletes first noted this paradoxical inconsistency of classical electrostatics for physical models that permit only a bounded density of positive charges. An approach was suggested to handle the physics of electrostatic charge distribution in a way that allows the imposition of a defined upper limit on positive charge density.

*Disclaimer: In this report we wish to consider the simplest approach to examine the situation where negative charges in a conductor are mobile and positive charges, when present, occur at a maximum (fixed) finite volumetric density. One may draw an analogy to the physical world by considering these charges to be the valence charges of a metallic conductor. However, while such an analogy may help provide mnemonic understanding to the present effort, our focus here is on the simple modeling approach and not the atomic analogy. Therefore, throughout the remainder of this report, we refer only to the model concepts of positive and negative charges, rather than to a physical atomistic interpretation of what that might mean.

We recall Fig. 1,* first presented in ARL-TR-8492.[2] In the electrically neutral Ω_n domain, the density of positive charges is exactly balanced by the density of mobile negative charges. However, unlike mobile negative charges, which are free to congregate on free-surface interfaces S_n with a finite surface density σ_{S_n} (a nonzero "surface density" implies an infinite volumetric density), the model posited that, instead, excess positive charges must be distributed through finite volumetric domains Ω_a that are void of mobile negative charges. Being void of negative charges, the volumetric-charge density in Ω_a domains is q_+, which can be considered a known material property of the conductor. Interfaces between the negative-charge-free Ω_a domain and the outer void (denoted S_a) and between the Ω_a and Ω_n domains (denoted Σ) are void of charges altogether, and thus, possess no surface-charge density, unlike S_n surfaces.

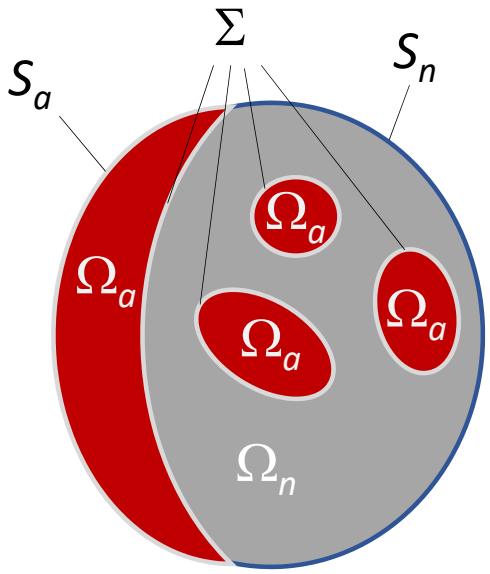

Fig. 1 Cross-sectional (cutaway) geometry of a conductor

In ARL-TR-8492,[2] the solution to these modified equations of classical electrostatics was demonstrated for the simple case of 1-D Cartesian geometry, to include the electric potential and the corresponding electric field distribution, as well as determining the location of the domain interfaces as a function of the excess charge,

*In this and the figures to follow, one may follow the heuristic rule-of-thumb that dark and light gray denote electrically neutral domains and interfaces, respectively; red denotes a domain void of negative charges and blue denotes an interface comprised solely of mobile negative charges and characterized by a surface-charge density.

positive or negative.

While solutions demonstrated in the prior reports are clear, the 1-D Cartesian-geometry case is a very special case of limited application, since it necessarily posits a plate geometry of infinite lateral extent. In this report, the 1-D (symmetric) spherical-geometry case is considered. This geometry has more realistic applications, in that spherical geometry will involve a finite total number of charges. Additionally, the electrostatic potential and field decay to zero at distant locations, far from the sphere.

2. Governing Equations

Let φ represent the electrostatic potential function over a given space. The variation of φ in space must satisfy the Poisson equation (employing the unit system of Landau and Lifshitz[3]):

$$\nabla^2\varphi = -4\pi q \quad , \tag{1}$$

where ∇^2 is the Laplacian operator. The term q is the local volumetric charge density. However, in addition to this, because of the ability for mobile negative charges to freely redistribute inside a conductor, we have the added constraint that, in any given neutral Ω_n domain, the potential φ must be a constant if the system is in electrostatic equilibrium (if the potential were to vary across a given Ω_n domain, mobile charges would immediately redistribute themselves in response).

The electric field $\mathbf{E}$ is given by $\mathbf{E} = -\nabla\varphi$. In all neutral Ω_n domains, therefore, the electric field $\mathbf{E}$ is identically zero. In the 1-D radially symmetric configuration of interest in this report, the gradient reduces to $\nabla\varphi = (d\varphi/dr)\,\hat{\mathbf{i}}$, where $\hat{\mathbf{i}}$ is the vector norm aligned with the radius of the coordinate system. Therefore, we have $\mathbf{E} = -(d\varphi/dr)\,\hat{\mathbf{i}}$ to describe the electric field for this symmetric geometry.

In the neutral Ω_n domain, where positive and negative charge densities are in balance, $q = 0$. In the Ω_a domain, void of negative charges and with a uniform density of positive charge, the value of q takes on the fixed positive charge density, so that $q = q_+$. In the domain external to the body, q should take on the local charge density. However, since we are here considering the external domain to be a void without charge, we once again find that $q = 0$ in the external domain. In addition, because the external domain is without charge density, the potential φ, far from the body, must approach zero.

2.1 Poisson Equation for a Spherical Geometry

In spherical (r, θ, ω) coordinates, the Laplacian operator is given as

$$\nabla^2\varphi = \frac{1}{r^2 \sin\theta}\left[\frac{\partial}{\partial r}\left(r^2 \sin\theta \frac{\partial\varphi}{\partial r}\right) + \frac{\partial}{\partial\theta}\left(\sin\theta\frac{\partial\varphi}{\partial\theta}\right) + \frac{\partial}{\partial\omega}\left(\frac{1}{\sin\theta}\frac{\partial\varphi}{\partial\omega}\right)\right] \quad .$$

For the limited case of spherical 1-D symmetry (spherical geometry) that we consider here, this reduces to

$$\nabla^2\varphi = \frac{1}{r^2}\frac{d}{dr}\left(r^2\frac{d\varphi}{dr}\right) \quad .$$

Consider, thus, the Poisson equation (Eq. 1) for this type of 1-D symmetry:

$$\frac{1}{r^2}\frac{d}{dr}\left(r^2\frac{d\varphi}{dr}\right) = -4\pi q \quad .$$

Integration (twice) provides the general 1-D solution for the case of spherical geometry,

$$\begin{aligned} \varphi(r) &= -\frac{2\pi}{3}qr^2 - \frac{M}{r} + N \\ \frac{d\varphi}{dr} &= -\frac{4\pi}{3}qr + \frac{M}{r^2} \end{aligned} \qquad \text{(subject to Table 1 constraints)} \quad . \qquad (2)$$

The solution embodied in Eq. 2 is employed in this report to calculate the electrostatic potential φ and the electric field magnitude ($E = -d\varphi/dr$) for various static spherical configurations involving a net charge imbalance between the positive charges that are fixed to the body with a constrained density (*e.g.*, a lattice) and mobile negative charges that are free to relocate in and over the body, without a constraining density.

The constraints on Eq. 2 are based both on the type of domain being considered as well as the domain's boundary. For example, $q = M = 0$ in Ω_n domains to ensure that the potential φ remains constant. Outside the external boundary, $N = 0$ to ensure a vanishing potential φ far from the body. Everywhere, but notably at the center of the sphere, the potential is bounded, $\varphi(0) < \infty$, implying that $M = 0$ for the domain that encompasses $r = 0$. A summary of the operational constraints on Eq. 2 is provided in Table 1.

Table 1 Domain constraints on Eq. 2

Constraint(s)	Domain
$q = 0$ $M = 0$	in (charge-neutral) Ω_n domain
$q = q_+$	in Ω_a domain
$q = q_{\text{ext}} = 0$	for the domain beyond external boundary S
$q = 0$	within any void (including internal voids)
$N = 0$	in the domain encompassing $r \to \infty$
$M = 0$	in the domain encompassing the point $r = 0$

The solutions presented in this report are in the context of the paradoxical inconsistency raised in earlier reports; namely, subject to the constrained volumetric charge density of positive ions.

2.2 Domain-Interface Continuity/Jump Conditions

In the problems of interest in this report, a spherical conductive body sits in a void. The body contains positive and/or negative charges that are distributed through the body in accordance with certain spherically symmetrical configurations to be considered later in this report. The charges are responsible for creating the electric potential φ, which obeys the general form of Eq. 2, subject to the boundary conditions of the particular configuration at hand.

However, all configurations share certain elements. The potential $\varphi(r)$ is everywhere continuous, even across domain interfaces, such that

$$\left[\varphi\right]_-^+ = 0 \qquad \text{across all interfaces.} \tag{3}$$

Across charge-free domain interfaces S_a and Σ, the electric field is continuous:

$$\left[\nabla\varphi\right]_-^+ \cdot \mathbf{n} = \left[\frac{d\varphi}{dr}\right]_-^+ = 0 \qquad \text{across } S_a \text{ and } \Sigma \text{ interfaces,} \tag{4}$$

where $\mathbf{n}$ is the local outward surface normal of the interface. The dot product reduces here to a simple derivative because, in this 1-D configuration, the gradient of φ and the surface normal $\mathbf{n}$ are both aligned with the radial coordinate, r. However, across S_n interfaces (infinitesimally thin layers containing finite charge), the electric

field is discontinuous:

$$\left[\nabla\varphi\right]_{-}^{+} \cdot \mathbf{n} = \left[\frac{d\varphi}{dr}\right]_{-}^{+} = -4\pi\sigma_{S_n} \qquad \text{across } S_n \text{ interfaces,} \tag{5}$$

where σ_{S_n} is the (negative) charge per unit area in the S_n surface-boundary layer.

2.3 Total Quantity of Charges

The existence of an electric potential and its associated field arise from the presence of negative and positive charges in the problem domain. We therefore require the ability to tally the amount of charge in the various configurations that follow (note that the balanced, covalently bound charges are not part of this tally). The negative charge tally was given by Eq. 11 in a predecessor report, ARL-TR-8492,[2]

$$Q_{-} = \int_{\Omega_n} d\Omega\, q_{-} + \int_{S_n} dS\, \sigma_{S_n} \quad .$$

But, because $q_{+} + q_{-} = 0$ in the neutral Ω_n domain, and knowing that q_{-} and σ_{S_n} are both negative in magnitude, this equation can be expressed as the *positive* tally of negative charges:

$$|Q_{-}| = \int_{\Omega_n} d\Omega\, q_{+} - \int_{S_n} dS\, \sigma_{S_n} \quad . \tag{6}$$

The corresponding tally for positive charge is

$$Q_{+} = \int_{\Omega_n} d\Omega\, q_{+} + \int_{\Omega_a} d\Omega\, q_{+} \quad . \tag{7}$$

There are no surface integrals in Eq. 7 because the various interfaces, S_a, S_n, and Σ, do not contain any positive charges to be tallied.

The net total charge in the system is simply

$$Q_{\text{net}} = Q_{+} - |Q_{-}| \quad , \tag{8}$$

which can be either positive or negative, depending on the preponderance of each type of charge.

3. 1-D Solutions for a Spherical Geometry

We now consider several charge distributions that might arise when a given Q_{net} is applied to a spherical conductor. To start, we consider only the simplest charge distributions, limiting topologies to a single instance each of any given domain type (Ω_n, Ω_a) and interface type (S_a, S_n, Σ). The only topologically plausible configurations for 1-D geometry are, initially, thus:

1. There is excess negative charge on the external S_n interface and no Ω_a domain (which is void of negative charge) exists in the body.

2. There is excess positive charge in the body (an Ω_a domain) and no S_n external boundary (harboring negative surface-charge density) exists.

3. There exist both an Ω_a domain void of negative charge as well as an S_n external boundary harboring negative surface-charge density.

In the case of Configuration 2, one could envision the Ω_a domain either centrally located or at the periphery of the sphere. However, for this configuration, only the instance of Ω_a on the periphery is considered, since the alternative of a central Ω_a domain is actually a special case of Configuration 3 (when $\sigma_{S_n} \rightarrow 0$). These three configurations of charge distribution examined in this report are the 1-D spherical-geometry analogs to the 1-D Cartesian-geometry examples given in ARL-TR-8492.[2]

3.1 Configuration 1

Consider the sphere presented in Fig. 2. This configuration represents the classical electrostatic case where all the *excess* charges are mobile and are concentrated on surfaces without regard to volumetric-charge-density limitation.

3.1.1 Charge Tally

From Eq. 6, the magnitude of negative charge in the system is

$$|Q_-| = \frac{4\pi}{3} R_s^3 q_+ - 4\pi R_s^2 \sigma_{S_n} \quad . \tag{9}$$

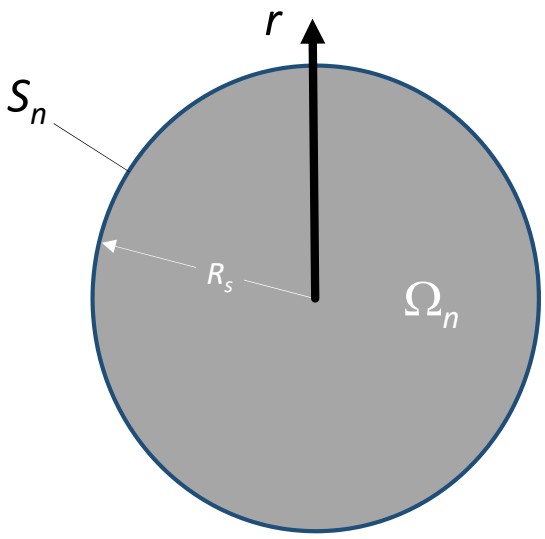

Fig. 2 Configuration 1, comprised solely of a neutral Ω_n domain (gray), with mobile negative charges concentrated at the external S_n boundary

From Eq. 7, the positive charge counterpart is

$$Q_+ = \frac{4\pi}{3} R_s^3 q_+ \tag{10}$$

resulting in a net charge of

$$Q_{\text{net}} = 4\pi R_s^2 \sigma_{S_n} < 0 \quad . \tag{11}$$

Reexpressing Eq. 11 as σ_{S_n} in terms of the given Q_{net} confirms the conclusion that the surface density of negative charge is simply the given net charge in the system per unit surface area of the sphere:

$$\sigma_{S_n} = \frac{Q_{\text{net}}}{4\pi R_s^2} \quad . \tag{12}$$

3.1.2 Electrostatic Potential and Electric Field

The equations that apply to each domain of Configuration 1 and the compatibility/jump equations that apply at interfaces between the domains are presented in Tables 2 and 3, respectively.

The negatively charged S_n interface has a nonzero surface-charge density, which produces a jump discontinuity in the electric field, across the sphere's S_n boundary,

Table 2 Configuration 1: equations by domain

	Region 1 Ω_n **domain (gray)** $(r < R_s)$	**Region 2 outer void** $(r > R_s)$
Constraints (see Table 1)	$q_1 = M_1 = 0$	$q_2 = N_2 = 0$
Governing equations (see Eq. 2)	$\varphi = N_1$ $\frac{d\varphi}{dr} = 0$	$\varphi = -\frac{M_2}{r}$ $\frac{d\phi_2}{dr} = \frac{M_2}{r^2}$
Boundary values at $r = R_s$	$\varphi(R_s) = N_1$ $\left.\frac{d\varphi}{dr}\right\|_{[R_s]^-} = 0$	$\varphi(R_s) = -\frac{M_2}{R_s}$ $\left.\frac{d\varphi}{dr}\right\|_{[R_s]^+} = \frac{M_2}{R_s^2}$

Table 3 Configuration 1: unknowns and interface continuity/jump equations

Unknowns	N_1 M_2	
S_n interface continuity/jump conditions (see Eqs. 3 and 5)	$\left[\varphi\right]_-^+ = 0$	at $r = R_s$
	$\left[\frac{d\varphi}{dr}\right]_-^+ = -4\pi\sigma_{S_n}$	at $r = R_s$

in accordance with Eq. 5. Thus, since $\left[d\varphi/dr\right]_{[R_s]^-} = 0$ on the interior of the S_n interface, the jump condition (Table 3) requires that $\left[d\varphi/dr\right]_{[R_s]^+} = -4\pi\sigma_{S_n}$ on the exterior of the S_n surface interface. Choosing the value of M_2 to satisfy the jump condition at $r = R_s$ leads to

$$\begin{aligned} \varphi &= 4\pi\frac{R_s^2\sigma_{S_n}}{r} \\ -\frac{d\varphi}{dr} &= 4\pi\frac{R_s^2\sigma_{S_n}}{r^2} \end{aligned} \qquad \text{for } r > R_s \quad . \tag{13}$$

Because φ must be continuous across the S_n interface, the value for N_1 may be determined for region 1:

$$\begin{aligned} \varphi &= 4\pi R_s\sigma_n \\ d\varphi/dr &= 0 \end{aligned} \qquad \text{for } r < R_s \quad . \tag{14}$$

3.1.3 Configuration 1: Final Result

These expressions, Eqs. 14 and 13, may be reexpressed in terms of the net charge, Q_{net}, given for this configuration, by Eq. 11:

$$\begin{aligned} \varphi &= \frac{Q_{\text{net}}}{R_s} \\ d\varphi/dr &= 0 \end{aligned} \qquad \text{for } r < R_s \tag{15}$$

and

$$\begin{aligned} \varphi &= \frac{Q_{\text{net}}}{r} \\ -\frac{d\varphi}{dr} &= \frac{Q_{\text{net}}}{r^2} \end{aligned} \qquad \text{for } r > R_s \quad . \tag{16}$$

Note that Eq. 16 is the well-known result that the potential outside of a charged sphere is proportional to the net charge and inversely proportional to the distance from the body center, in the manner of a point charge.

On the external S_n boundary, the potential and field take on the values

$$\begin{aligned} \varphi(R_s) &= \frac{Q_{\text{net}}}{R_s} \\ -\left[\frac{d\varphi}{dr}\right]^+ &= \frac{Q_{\text{net}}}{R_s^2} \end{aligned} \qquad \text{on the } S_n \text{ boundary at } r = \left[R_s\right]^+ \quad . \tag{17}$$

A sample potential illustrating the Configuration 1 charge distribution is given in Fig. 3.

3.2 Configuration 2

Consider the sphere presented in Fig. 4. There are three regions and two boundaries. The location of the internal Σ boundary is determined by how many mobile negative charges are present in the system.

3.2.1 Charge Tally

One may apply the charge tallies given by Eqs. 6 and 7 to Configuration 2. Concerning negative charges, there are no S_n boundaries in this configuration, and so all mobile electrons are confined to the gray Ω_n domain. The tally of mobile negative charges, therefore, proceeds as

$$|Q_-| = \frac{4\pi}{3} R_\Sigma^3 q_+ \quad .$$

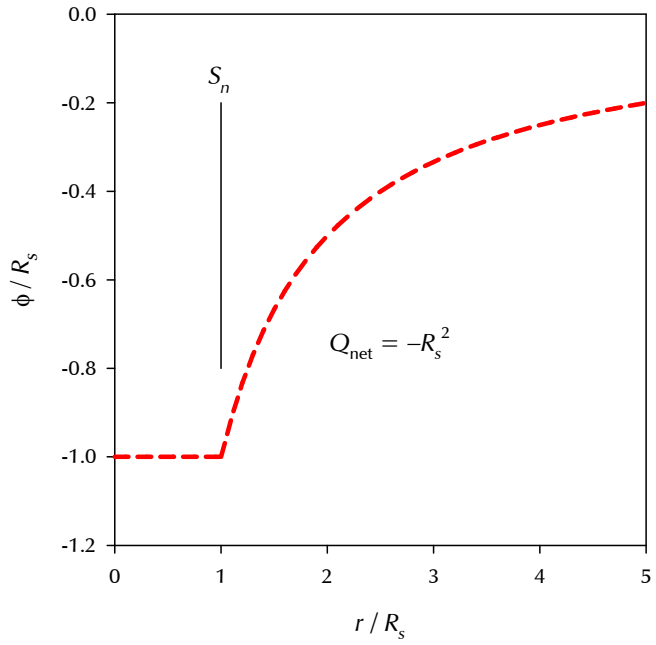

Fig. 3 Configuration 1 potential $\varphi(r)$, for the case where $Q_{\text{net}} = -R_s^2$

In a similar fashion, the positive charges in the body are evenly distributed throughout the body, both in Ω_n and Ω_a, at a density of q_+, and so the tally becomes

$$Q_+ = \frac{4\pi}{3} R_a^3 q_+ \quad .$$

The net charge is simply $Q_+ - |Q_-|$, which for this configuration, results in

$$Q_{\text{net}} = \frac{4\pi}{3}(R_a^3 - R_\Sigma^3) q_+ > 0 \quad . \tag{18}$$

Therefore, the volumetric density of positive charge q_+ can be expressed in terms of the various charge tallies:

$$q_+ = \frac{3Q_{\text{net}}}{4\pi(R_a^3 - R_\Sigma^3)} = \frac{3|Q_-|}{4\pi R_\Sigma^3} = \frac{3Q_+}{4\pi R_a^3} \quad . \tag{19}$$

We may solve for the location of the Σ interface with Eq. 19, in terms of the given net charge Q_{net} or, alternately, the ratio of mobile negative charges (Q_-) to positive charges (Q_+):

$$R_\Sigma = \sqrt[3]{R_a^3 - \frac{3Q_{\text{net}}}{4\pi q_+}} = R_a \sqrt[3]{\frac{|Q_-|}{Q_+}} \quad . \tag{20}$$

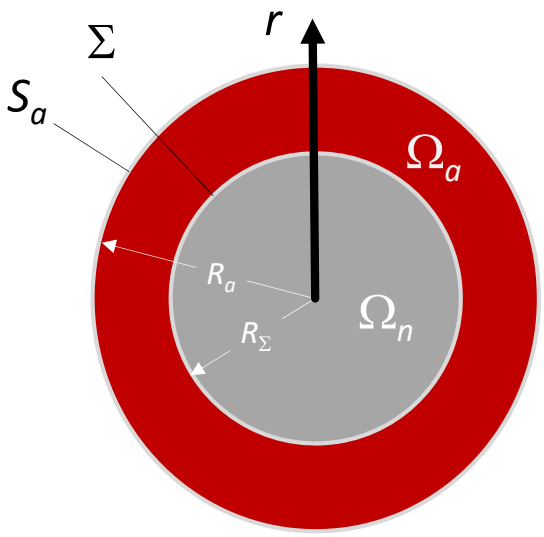

Fig. 4 Configuration 2, with finite Ω_a domain (red) at the external boundary

3.2.2 Electrostatic Potential and Electric Field

The equations that apply to each domain of Configuration 2 and the compatibility/jump equations that apply at interfaces between the domains are presented in Tables 4 and 5, respectively. We do not list R_Σ as an unknown, since it is fully determined given the specification of Q_{net}, by way of Eq. 20, in light of the material property of the conductor, q_+.

In Configuration 2, both interfaces (S_a and Σ) are without surface-charge density. Therefore, they will produce no discontinuities in $d\varphi/dr$ across their respective boundaries. The potential φ will be continuous, as well, in accordance with Eqs. 3 and 4, as shown in Table 5.

Consider region 1 (the gray Ω_n domain), which we signify using a corresponding subscript on the constant terms q, M, and N of Eq. 2. We know that both $q_1 = 0$ and $M_1 = 0$ in Ω_n domains. The integration constant N_1, while yet unknown in its value, is all that remains of the region 1 solution, as seen in Table 4.

We denote the outer void as region 3, with a corresponding subscript. At the S_a boundary, we note (even with M_3 as yet undetermined) that

$$\varphi(R_a) = -R_a \left.\frac{d\varphi}{dr}\right|_{R_a} \quad . \tag{21}$$

Table 4 Configuration 2: equations by domain

	Region 1 **Ω_n domain (gray)** $(r \le R_\Sigma)$	**Region 2** **Ω_a domain (red)** $(R_\Sigma < r \le R_a)$	**Region 3** **outer void** $(r > R_a)$
Constraints (see Table 1)	$q_1 = M_1 = 0$	$q_2 = q_+$	$q_3 = N_3 = 0$
Governing equations (see Eq. 2)	$\varphi = N_1$ $\dfrac{d\varphi}{dr} = 0$	$\varphi = -\dfrac{2\pi}{3} q_2 r^2 - \dfrac{M_2}{r} + N_2$ $\dfrac{d\varphi}{dr} = -\dfrac{4\pi}{3} q_2 r + \dfrac{M_2}{r^2}$	$\varphi = -\dfrac{M_3}{r}$ $\dfrac{d\phi_3}{dr} = \dfrac{M_3}{r^2}$
Boundary values at $r = R_\Sigma$	$\varphi(R_\Sigma) = N_1$ $\left.\dfrac{d\varphi}{dr}\right\|_{R_\Sigma} = 0$	$\varphi(R_\Sigma) = -\dfrac{2\pi}{3} q_2 R_\Sigma^2 - \dfrac{M_2}{R_\Sigma} + N_2$ $\left.\dfrac{d\varphi}{dr}\right\|_{R_\Sigma} = -\dfrac{4\pi}{3} q_2 R_\Sigma + \dfrac{M_2}{R_\Sigma^2}$	
Boundary values at $r = R_a$		$\varphi(R_a) = -\dfrac{2\pi}{3} q_2 R_a^2 - \dfrac{M_2}{R_a} + N_2$ $\left.\dfrac{d\varphi}{dr}\right\|_{R_a} = -\dfrac{4\pi}{3} q_2 R_a + \dfrac{M_2}{R_a^2}$	$\varphi(R_a) = -\dfrac{M_3}{R_a}$ $\left.\dfrac{d\varphi}{dr}\right\|_{R_a} = \dfrac{M_3}{R_a^2}$

Table 5 Configuration 2: unknowns and interface continuity/jump equations

Unknowns	N_1 M_2 N_2 M_3	
Σ interface continuity conditions (see Eqs. 3 and 4)	$\left[\varphi\right]_-^+ = 0$	at $r = R_\Sigma$
	$\left[\dfrac{d\varphi}{dr}\right]_-^+ = 0$	at $r = R_\Sigma$
S_a interface continuity conditions (see Eqs. 3 and 4)	$\left[\varphi\right]_-^+ = 0$	at $r = R_a$
	$\left[\dfrac{d\varphi}{dr}\right]_-^+ = 0$	at $r = R_a$

Finally, we come to region 2, encompassing the red Ω_a domain. To provide continuity in $d\varphi/dr$ at $r = R_\Sigma$, we require that

$$-\frac{4\pi}{3} q_2 R_\Sigma + \frac{M_2}{R_\Sigma^2} = 0 \quad .$$

Thus,

$$M_2 = \frac{4\pi}{3} q_2 R_\Sigma^3$$

must hold. Substituting this value into the potential and field, as the Ω_a domain approaches the S_a interface at $r = R_a$,

$$\begin{aligned} \varphi(R_a) &= -\frac{2\pi q_2 R_a^2}{3} - \frac{4\pi q_2 R_\Sigma^3}{3R_a} + N_2 \\ \left.\frac{d\varphi}{dr}\right|_{R_a} &= -\frac{4\pi q_2 R_a}{3} + \frac{4\pi q_2 R_\Sigma^3}{3R_a^2} \end{aligned} \quad . \tag{22}$$

Because there is zero surface-charge density at the S_a boundary, there is no discontinuity in φ and $d\varphi/dr$ at the interface between Ω_a and the outer void. Therefore, replacing the terms of Eq. 21 with those obtained in Eq. 22 gives

$$-\frac{2\pi q_2 R_a^2}{3} - \frac{4\pi q_2 R_\Sigma^3}{3R_a} + N_2 = +\frac{4\pi q_2 R_a^2}{3} - \frac{4\pi q_2 R_\Sigma^3}{3R_a} \quad .$$

From this, we determine the value of N_2 as

$$N_2 = 2\pi q_2 R_a^2 \quad .$$

We also know that $q_2 = q_+$. Therefore, the solution in Ω_a (region 2), with all constants now known, is

$$\begin{aligned} \varphi &= 4\pi\left(\frac{R_a^2}{2} - \frac{r^2}{6} - \frac{R_\Sigma^3}{3r}\right) q_+ \\ -\frac{d\varphi}{dr} &= \frac{4\pi}{3}\left(r - \frac{R_\Sigma^3}{r^2}\right) q_+ \end{aligned} \qquad \text{for } R_\Sigma < r \le R_a \quad . \tag{23}$$

The value of φ from Eq. 23, evaluated at $r = R_\Sigma$ (the Σ boundary) may be used to

enforce continuity with the Ω_n domain (region 1):

$$\begin{aligned} \varphi &= 2\pi(R_a^2 - R_\Sigma^2)q_+ \\ -\frac{d\varphi}{dr} &= 0 \end{aligned} \qquad \text{for } r \le R_\Sigma \quad . \tag{24}$$

Likewise, the value of φ from Eq. 23, evaluated at $r = R_a$ (the S_a boundary), may be used to enforce continuity with the outer void (region 3) in solving for M_3:

$$M_3 = -\frac{4\pi}{3}(R_a^3 - R_\Sigma^3)q_+ \quad .$$

Thus, the solution in the outer void (region 3) becomes

$$\begin{aligned} \varphi &= \frac{4\pi}{3}(R_a^3 - R_\Sigma^3)\frac{q_+}{r} \\ -\frac{d\varphi}{dr} &= \frac{4\pi}{3}(R_a^3 - R_\Sigma^3)\frac{q_+}{r^2} \end{aligned} \qquad \text{for } r > R_a \quad . \tag{25}$$

3.2.3 Configuration 2: Final Result

The solutions given by Eqs. 24, 23, and 25 may be expressed in terms of the cumulative charge through the elimination of q_+, using Eq. 19:

$$\begin{aligned} \varphi &= \frac{3Q_{\text{net}}(R_a^2 - R_\Sigma^2)}{2(R_a^3 - R_\Sigma^3)} \\ -\frac{d\varphi}{dr} &= 0 \end{aligned} \qquad \text{for } r \le R_\Sigma \quad , \tag{26}$$

$$\begin{aligned} \varphi &= \frac{3Q_{\text{net}}}{R_a^3 - R_\Sigma^2}\left(\frac{R_a^2}{2} - \frac{r^2}{6} - \frac{R_\Sigma^3}{3r}\right) \\ -\frac{d\varphi}{dr} &= \frac{Q_{\text{net}}}{R_a^3 - R_\Sigma^2}\left(r - \frac{R_\Sigma^3}{r^2}\right) \end{aligned} \qquad \text{for } R_\Sigma < r \le R_a \quad , \tag{27}$$

$$\begin{aligned} \varphi &= \frac{Q_{\text{net}}}{r} \\ -\frac{d\varphi}{dr} &= \frac{Q_{\text{net}}}{r^2} \end{aligned} \qquad \text{for } r > R_a \quad . \tag{28}$$

Just as in the case of Configuration 1, Eq. 28 reproduces the well-known result that the potential outside of a charged sphere is proportional to the net charge and inversely proportional to the distance from the body center, in the manner of a point

charge. This result is valid even though the distribution of excess charge is not confined to an infinitesimally thin surface layer, as in the case of Configuration 1.

Equations 26–28 solve for the potential φ and its spatial derivative within regions 1–3, respectively. The values of the potential and its associated field at the region interfaces are given as

$$\varphi(R_\Sigma) = \frac{3Q_{\text{net}}(R_a^2 - R_\Sigma^2)}{2(R_a^3 - R_\Sigma^3)} \qquad \text{on the } \Sigma \text{ boundary at } r = R_\Sigma \qquad (29)$$
$$-\left.\frac{d\varphi}{dr}\right|_{R_\Sigma} = 0$$

and

$$\varphi(R_a) = \frac{Q_{\text{net}}}{R_a} \qquad \text{on the } S_a \text{ boundary at } r = R_a \quad . \qquad (30)$$
$$-\left.\frac{d\varphi}{dr}\right|_{R_a} = \frac{Q_{\text{net}}}{R_a^2}$$

A sample potential illustrating the Configuration 2 charge distribution is given in Fig. 5.

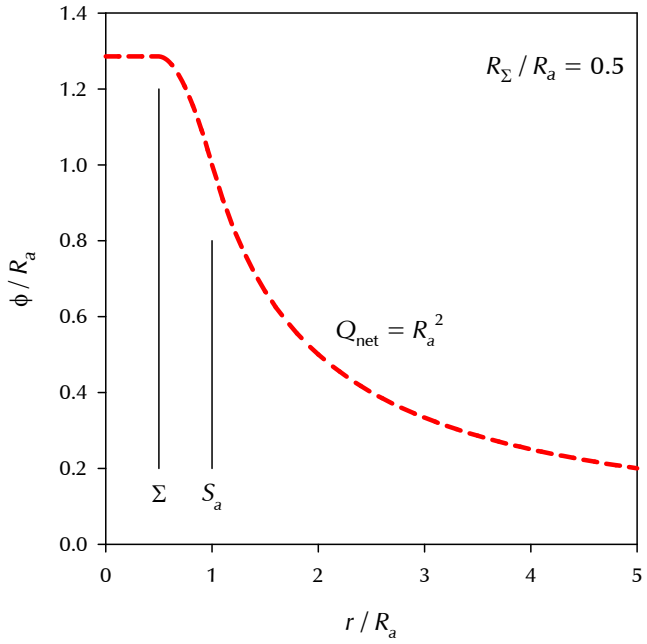

Fig. 5 Configuration 2 potential $\varphi(r)$, for the case where $Q_{\text{net}} = R_s^2$

3.3 Configuration 3

Consider the sphere presented in Fig. 6. There are three regions and two boundaries. This configuration is analogous to that of Configuration 2, but with the sense of the domains reversed. Of course, with a S_n interface on the sphere's exterior, the possibility of a negative surface charge must be considered with the case.

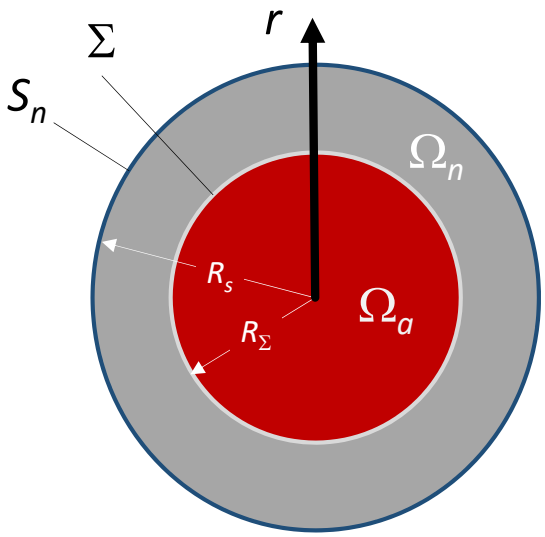

Fig. 6 Configuration 3, with finite Ω_a domain (red) at the sphere center boundary

3.3.1 Charge Tally

As with other configurations, one may apply the charge tallies given by Eqs. 6 and 7 to Configuration 3. The negative and positive charge tallies are

$$|Q_-| = \frac{4\pi}{3}(R_s^3 - R_\Sigma^3)q_+ - 4\pi R_s^2 \sigma_{S_n}$$
$$Q_+ = \frac{4\pi}{3} R_s^3 q_+$$

The net charge of the configuration is

$$Q_{\text{net}} = \frac{4\pi}{3} R_\Sigma^3 q_+ + 4\pi R_s^2 \sigma_{S_n}$$

The size of the negative-charge-free zone may be solved as

$$R_\Sigma = \sqrt[3]{\frac{3}{4\pi q_+}\left(Q_{\text{net}} - 4\pi R_s^2 \sigma_{S_n}\right)} \quad . \tag{31}$$

Something is already unnerving with this expression for a conductive sphere of radius R_s. Namely, for a given net charge and positive charge density, Q_{net} and q_+, respectively, there is not a unique configuration of σ_{S_n} and R_Σ associated with it. How does the geometry "know" what charge distribution to assume for a given charge imbalance, Q_{net}? We proceed, nonetheless.

3.3.2 Electrostatic Potential and Electric Field

The equations that apply to each domain of Configuration 3 and the compatibility/jump equations that apply at interfaces between the domains are presented in Tables 6 and 7, respectively. The value of R_Σ remains an unknown because it is not determinable from Eq. 31, given the initial condition of Q_{net} (since σ_{S_n} is *a priori* unknown).

We sense an immediate problem when we look at the continuity of $d\varphi/dr$ at the Σ interface (see Tables 6 and 7 highlighted in red). There can be no jump in $d\varphi/dr$ across the Σ interface. But, as the Ω_a domain (region 1) approaches the interface at $r = R_\Sigma$, we have that $d\varphi/dr\big|_{R_\Sigma} = -4\pi q_1 R_\Sigma/3 < 0$. In contrast, throughout the Ω_n domain (region 2), we have $d\varphi/dr\big|_{R_\Sigma} = 0$.

For any value of R_Σ other than $R_\Sigma = 0$, these two conditions are incompatible and, therefore, Configuration 3 does not represent an admissible electrostatic charge configuration. If the value of Q_{net} is negative, the charge distribution will, instead, assume that of Configuration 1. If positive, some other configuration will be required, perhaps that already addressed as Configuration 2.

3.4 Configuration 3a

One ponders the inadmissibility of Configuration 3, and considers, for the case when Q_{net} is positive, whether a variation of it might eliminate the cited incompatibility. For example, if the Ω_a domain were not centrally located, but instead positioned *between* two Ω_n domains, as in Fig. 7, the Poisson solution in that domain would not require that $M = 0$. In particular, the general form of solution in the Ω_a domain would be

$$\begin{aligned} \varphi &= \frac{2\pi}{3} r^2 q_+ - \frac{M}{r} + N \\ \frac{d\varphi}{dr} &= \frac{4\pi}{3} r q_+ + \frac{M}{r^2} \end{aligned} \quad . \tag{32}$$

Table 6 Configuration 3: equations by domain

	Region 1 **Ω_a domain (red)** $(r \le R_\Sigma)$	**Region 2** **Ω_n domain (gray)** $(R_\Sigma < r \le R_s)$	**Region 3** **outer void** $(r > R_s)$
Constraints (see Table 1)	$q_1 = q_+ \quad M_1 = 0$	$q_2 = M_2 = 0$	$q_3 = N_3 = 0$
Governing equations (see Eq. 2)	$\varphi = -\frac{2\pi}{3} q_1 r^2 + N_1$ $\frac{d\varphi}{dr} = -\frac{4\pi}{3} q_1 r$	$\varphi = N_2$ $\frac{d\varphi}{dr} = 0$	$\varphi = -\frac{M_3}{r}$ $\frac{d\phi}{dr} = \frac{M_3}{r^2}$
Boundary values at $r = R_\Sigma$	$\varphi(R_\Sigma) = -\frac{2\pi}{3} q_1 R_\Sigma^2 + N_1$ $\left.\frac{d\varphi}{dr}\right\|_{R_\Sigma} = -\frac{4\pi}{3} q_1 R_\Sigma$	$\varphi(R_\Sigma) = N_2$ $\left.\frac{d\varphi}{dr}\right\|_{R_\Sigma} = 0$	
Boundary values at $r = R_s$		$\varphi(R_s) = N_2$ $\left.\frac{d\varphi}{dr}\right\|_{[R_s]^-} = 0$	$\varphi(R_s) = -\frac{M_3}{R_s}$ $\left.\frac{d\varphi}{dr}\right\|_{[R_s]^+} = \frac{M_3}{R_s^2}$

Table 7 Configuration 3: unknowns and interface continuity/jump equations

Unknowns	N_1 N_2 M_3 R_Σ	
Σ interface continuity conditions (see Eqs. 3 and 4)	$\left[\varphi\right]_-^+ = 0$	at $r = R_\Sigma$
	$\left[\frac{d\varphi}{dr}\right]_-^+ = 0$	at $r = R_\Sigma$
S_n interface continuity/jump conditions (see Eqs. 3 and 5)	$\left[\varphi\right]_-^+ = 0$	at $r = R_s$
	$\left[\frac{d\varphi}{dr}\right]_-^+ = -4\pi\sigma_{S_n}$	at $r = R_s$

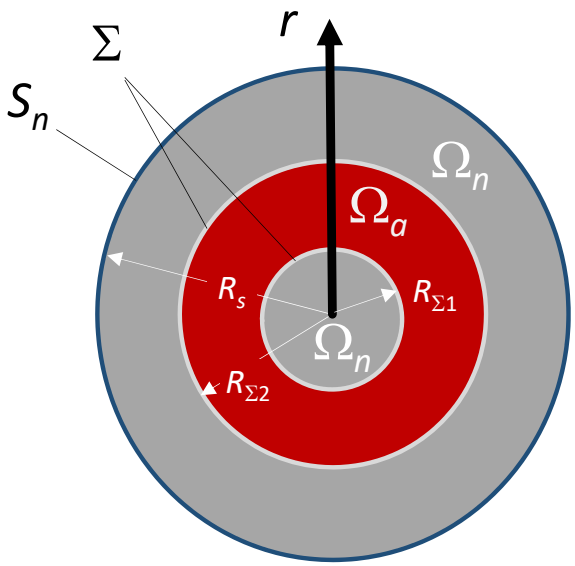

Fig. 7 Configuration 3a, with Ω_a domain (red) sandwiched between two neutral Ω_n domains

While Eq. 32 offers a greater number of fittable constants in the Ω_a domain than does Configuration 3, there are also different constraints, as well. Because the potential is constant in both adjacent Ω_n domains, the slope $d\varphi/dr = 0$ must hold true at both $r = R_{\Sigma 1}$ as well as $r = R_{\Sigma 2}$. Examining Eq. 32, to see when the condition $d\varphi/dr = 0$ can be satisfied, leads to the equation

$$r^3 = \frac{3M}{4\pi q_+} \qquad \text{when } d\varphi/dr = 0. \tag{33}$$

Equation 33 has at most one real solution for r and, therefore, one must conclude that it is not possible to simultaneously satisfy the requirement $d\varphi/dr = 0$ at both $r = R_{\Sigma 1}$ and $r = R_{\Sigma 2}$. Thus, Configuration 3a is likewise inadmissible.

3.5 Configuration 3b

The inadmissibility of Configuration 3 was driven by an unsatisfied requirement that $d\varphi/dr = 0$, at the Σ interface(s) of the Ω_a domain. As a hypothetical exercise, let us consider modifying the geometry of Configuration 3 to convert the Σ interface into an S_a interface. Such a modification would eliminate the troublesome $d\varphi/dr = 0$ requirement at the (former) Σ boundary of Ω_a.

This modification can be accomplished by removing the conductor material over the

domain (formerly $R_\Sigma < r < R_s$) and replacing it with void. However, an infinitesimally thin shell of conductor material is permitted to remain at $r = R_s$, with the explicit purpose of containing the excess negative surface charge originally postulated in Configuration 3. In practical terms, this replacement of conductor material with void has the effect of preventing any field-driven movement of mobile negative charges from the S_n interface toward the Ω_a domain. This revised configuration is depicted in Fig. 8.

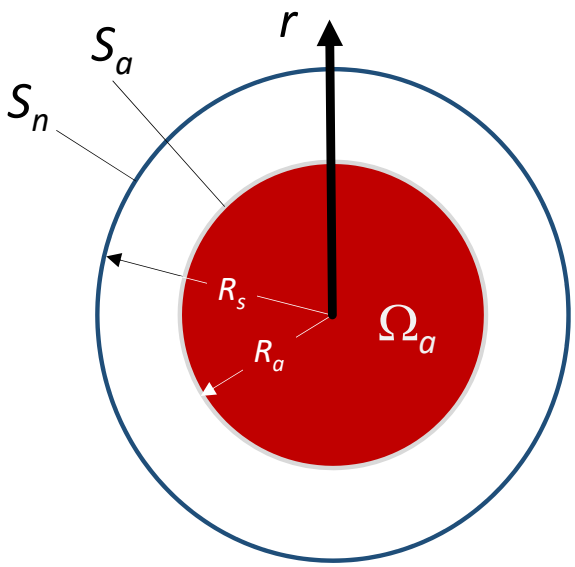

Fig. 8 Configuration 3b, with internal void between Ω_a domain (red) and an infinitesimally thin S_n interface

3.5.1 Charge Tally

As with other configurations, one may apply the charge tallies given by Eqs. 6 and 7 to Configuration 3b. The negative and positive charge tallies are

$$|Q_-| = -4\pi R_s^2 \sigma_{S_n}$$
$$Q_+ = \frac{4\pi}{3} R_a^3 q_+ \quad .$$

The net charge of the configuration is, therefore,

$$Q_{\text{net}} = 4\pi \left(\frac{R_a^3 q_+}{3} + R_s^2 \sigma_{S_n} \right) \quad .$$

Not surprisingly, the net charge for Configuration 3b exactly parallels the value calculated for Configuration 3, which differs from the present case only in that the neutral conductor has been replaced with an interior void (thus, the unknown R_Σ is redesignated here as the given R_a).

Because R_a is now a given quantity, the value for Q_+ is explicitly known *a priori*. Since Q_{net} is also a given quantity, the value of Q_- and hence σ_{S_n} are also immediately derivable from the charge-tally equations.

3.5.2 Electrostatic Potential and Electric Field

The equations that apply to each domain of Configuration 3b and the compatibility/jump equations that apply at interfaces between the domains are presented in Tables 8 and 9, respectively. Other than the redesignation of R_Σ as R_a, there is only one difference in the equations between this configuration and the original Configuration 3 (Tables 6 and 7). In Configuration 3, Σ was an internal boundary whose exact location was to be determined, whereas, in the present case, R_a conforms to the specified body geometry. Therefore, in the present case, the constant M_2 replaces R_Σ as an unknown quantity.

The solution may be obtained in the following sequence: first, substitute into the $[d\varphi/dr]^+_-$ interface condition at $r = R_s$:

$$\frac{M_3 - M_2}{R_s^2} = -4\pi\sigma_{S_n} \quad . \tag{34}$$

Likewise, substitute into the $[\varphi]^+_-$ interface condition at $r = R_s$:

$$-\frac{M_2}{R_s} + N_2 = -\frac{M_3}{R_s} \quad . \tag{35}$$

Solve Eq. 35 for $M_3 - M_2$,

$$M_3 - M_2 = -R_s N_2 \quad , \tag{36}$$

and substitute it into Eq. 34 to isolate the value of N_2 as

$$N_2 = 4\pi\sigma_{S_n} R_s \qquad (< 0) \quad . \tag{37}$$

Table 8 Configuration 3b: equations by domain

	Region 1 **Ω_a domain (red)** $(r \le R_a)$	**Region 2** **inner void** $(R_a < r \le R_s)$	**Region 3** **outer void** $(r > R_s)$
Constraints (see Table 1)	$q_1 = q_+ \quad M_1 = 0$	$q_2 = 0$	$q_3 = N_3 = 0$
Governing equations (see Eq. 2)	$\varphi = -\frac{2\pi}{3} q_1 r^2 + N_1$ $\frac{d\varphi}{dr} = -\frac{4\pi}{3} q_1 r$	$\varphi = -\frac{M_2}{r} + N_2$ $\frac{d\varphi}{dr} = \frac{M_2}{r^2}$	$\varphi = -\frac{M_3}{r}$ $\frac{d\phi}{dr} = \frac{M_3}{r^2}$
Boundary values at $r = R_a$	$\varphi(R_a) = -\frac{2\pi}{3} q_1 R_a^2 + N_1$ $\left.\frac{d\varphi}{dr}\right\|_{R_a} = -\frac{4\pi}{3} q_1 R_a$	$\varphi(R_a) = -\frac{M_2}{R_a} + N_2$ $\left.\frac{d\varphi}{dr}\right\|_{R_a} = \frac{M_2}{R_a^2}$	
Boundary values at $r = R_s$		$\varphi(R_s) = -\frac{M_2}{R_s} + N_2$ $\left.\frac{d\varphi}{dr}\right\|_{[R_s]^-} = \frac{M_2}{R_s^2}$	$\varphi(R_s) = -\frac{M_3}{R_s}$ $\left.\frac{d\varphi}{dr}\right\|_{[R_s]^+} = \frac{M_3}{R_s^2}$

Table 9 Configuration 3b: unknowns and interface continuity/jump equations

Unknowns	$N_1 \quad M_2 \quad N_2 \quad M_3$	
S_a interface continuity conditions (see Eqs. 3 and 4)	$\left[\varphi\right]_-^+ = 0$	at $r = R_a$
	$\left[\frac{d\varphi}{dr}\right]_-^+ = 0$	at $r = R_a$
S_n interface continuity/jump conditions (see Eqs. 3 and 5)	$\left[\varphi\right]_-^+ = 0$	at $r = R_s$
	$\left[\frac{d\varphi}{dr}\right]_-^+ = -4\pi\sigma_{S_n}$	at $r = R_s$

Next, substitute into the $[d\varphi/dr]^+_-$ interface condition at $r = R_a$ and solve for M_2:

$$M_2 = -\frac{4\pi}{3} R_a^3 q_+ \qquad (< 0) \quad . \tag{38}$$

Equation 38 may be substituted into Eq. 36 to obtain M_3 as

$$M_3 = -4\pi\left(\frac{R_a^3 q_+}{3} + R_s^2 \sigma_{S_n}\right) \qquad (= -Q_{\text{net}}) \quad . \tag{39}$$

Lastly, one may substitute into the $[\varphi]^+_-$ interface condition at $r = R_a$ and solve the resulting equation for the last remaining unknown constant, N_1:

$$N_1 = 4\pi\left(\frac{R_a^2 q_+}{2} + R_s \sigma_{S_n}\right) \quad . \tag{40}$$

With all the unknowns now determined, the solutions present themselves. We have for region 1,

$$\begin{aligned} \varphi &= 4\pi\left(-\frac{r^2 q_+}{6} + \frac{R_a^2 q_+}{2} + R_s \sigma_{S_n}\right) \\ -\frac{d\varphi}{dr} &= \frac{4\pi}{3} r q_+ \end{aligned} \qquad \text{for } r \le R_a \quad ,$$

region 2,

$$\begin{aligned} \varphi &= 4\pi\left(\frac{R_a^3 q_+}{3r} + R_s \sigma_{S_n}\right) \\ -\frac{d\varphi}{dr} &= \frac{4\pi R_a^3 q_+}{3r^2} \end{aligned} \qquad \text{for } R_a < r < R_s \quad ,$$

and region 3,

$$\begin{aligned} \varphi &= 4\pi\left(\frac{R_a^3 q_+}{3r} + \frac{R_s^2 \sigma_{S_n}}{r}\right) \\ -\frac{d\phi}{dr} &= 4\pi\left(\frac{R_a^3 q_+}{3r^2} + \frac{R_s^2 \sigma_{S_n}}{r^2}\right) \end{aligned} \qquad \text{for } r > R_s \quad .$$

3.5.3 Configuration 3b: Final Result

The preceding results can be reexpressed to eliminate q_+ and σ_{S_n} in favor of the given charge tallies. In the Ω_a domain of region 1, we have

$$\varphi = \frac{1}{2}\left[3 - \left(\frac{r}{R_a}\right)^2\right] \frac{Q_+}{R_a} - \frac{|Q_-|}{R_s} \qquad \text{for } r \le R_a \quad .$$

In the inner void of region 2, we obtain

$$\varphi = \frac{Q_+}{r} - \frac{|Q_-|}{R_s} \qquad \text{for } R_a < r < R_s \quad .$$

Note that, in the outer void region, we recover the well-known result that

$$\varphi = \frac{Q_{\text{net}}}{r} \qquad \text{for } r > R_s.$$

Three sample potentials illustrating the Configuration 3b charge distribution are given in Fig. 9.

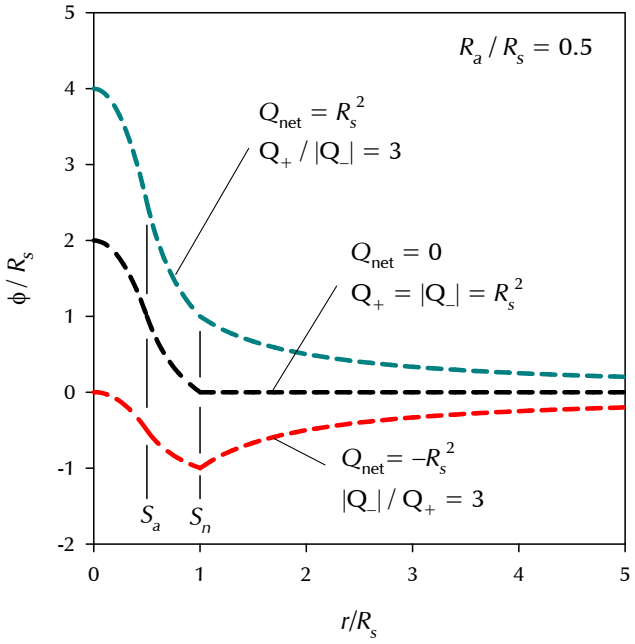

Fig. 9 Configuration 3b potential $\varphi(r)$, for three cases spanning $Q_{\text{net}} > 0$, $Q_{\text{net}} = 0$, and $Q_{\text{net}} < 0$

This hypothetical configuration was admittedly based on the existence of an infinitesimally thin, negatively charged shell at $r = R_s$. A proper analysis would solve the problem treating the shell with a thickness measurably greater than zero. That is not done here, because the focus was on a direct comparison to the untenable Configuration 3.

Here, the derivative of φ was negative at $r = R_a$, allowed by virtue of the fact that $r = R_a$ corresponds to an S_a (free surface) interface, rather than a Σ (interior) interface. What this result tells us is that if, through some miraculous means, the inner

void were instantly replaced with conductor material, the electrostatic equilibrium would be broken and mobile negative charges would flow from the S_n shell to fill the Ω_a region.

If the Q_{net} were negative, the Ω_a domain would be consumed and there would remain a smaller number of negative charges along the original S_n interface (establishing Configuration 1). If the Q_{net} were positive, the S_n interface would become depleted of surface charges and additional mobile negative charges would continue to move from the outer periphery of the Ω_n domain toward the sphere center, so as to fully consume the central Ω_a domain. A new Ω_a domain would form at the sphere periphery, taking over volume vacated by the mobile negative charges that migrated to the sphere center (establishing Configuration 2).

4. Conclusion

In an earlier report,[1] we demonstrated the paradoxical inconsistency of classical electrostatics for models permitting only a finite density of positive charges. A modification to the classical approach was needed to address this paradox. Such a modification was introduced in a second report.[2] Minimizing the complexification of the effort, the new physical mechanism introduced was a volumetric domain void of negative mobile charges (*e.g.*, Ω_a in our nomenclature). Associated with this domain is a new material constant, the maximum allowed positive-charge density, q_+.

In that report,[2] hypothetical charge distributions were examined and solved using the new modeling approach for problems involving 1-D Cartesian geometry. This report takes the modeling approach and extends the application to problems of 1-D spherical geometry, solving for various charge distributions in spherical conductors.

The results proved consistent with, not only the 1-D Cartesian solutions, but also what is already known for the classical model of electrostatics. Namely, excess charge in a spherical conductor will establish itself toward the exterior periphery of the body, regardless of whether the charge sits wholly on the body surface (a charged S_n interface for mobile negative charges) or is distributed through a charged volumetric domain (Ω_a for excess positive charge). Further, the established result was confirmed, that the potential outside of a charged sphere is proportional to the net charge and inversely proportional to the radial coordinate. This latter observa-

tion holds true whether the charge distribution manifests as a surface-charge density (σ_{S_n}) or as a distributed volumetric charge (q_+).

This consistency with classical theory is essential in the validation of the modified approach. At the same time, the modified approach avoids the situation of excess positive charge being distributed with infinite volumetric density across the surface of a body. Not only does such a change conform to what we know physically about the nature of crystalline conductors, but it also provides remedial hope in addressing the nagging challenge of modeling what would otherwise be physical discontinuities in a discretized domain.

5. References

1. Grinfeld M, Segletes SB. Toward paradoxical inconsistency in electrostatics of metallic conductors. Aberdeen Proving Ground (MD): Army Research Laboratory (US); 2018 May. Report No.: ARL-TR-8365.

2. Grinfeld M, Segletes SB. Consistent electrostatics of crystalline conductors. Aberdeen Proving Ground (MD): Army Research Laboratory (US); 2018 Sep. Report No.: ARL-TR-8492.

3. Landau LD, Lifshitz EM. Electrodynamics of continuous media. Oxford (UK): Pergamon; 1960.

1 (PDF) DEFENSE TECHNICAL INFORMATION CTR DTIC OCA

2 (PDF) DIR ARL
IMAL HRA
RECORDS MGMT
RDRL DCL
TECH LIB

1 (PDF) GOVT PRINTG OFC
A MALHOTRA

1 (PDF) COMMANDER
US ARMY ARDEC
R FONG

1 (PDF) NSWC
INDIAN HEAD DIVISION
T P MCGRATH II

1 (PDF) NAVAIR
E SIEVEKA

1 (PDF) US ARMY ERDEC
J Q EHRGOTT JR

3 (PDF) SANDIA NATL LAB
J NIEDERHAUS
A ROBINSON
C SIEFERT

2 (PDF) JOHNS HOPKINS UNIV
K RAMESH
L GRAHAM-BRADY

1 (PDF) DREXEL UNIVERSITY
B FAROUK

3 (PDF) DE TECHNOLOGIES
R CICCARELLI
W FLIS
W CLARK

ABERDEEN PROVING GROUND

61 (PDF) DIR USARL
RDRL VTM
M HAILE
RDRL WM
J MCCAULEY
S SCHOENFELD
RDRL WML C
K MCNESBY
B ROOS
RDRL WML H
L MAGNESS
C MEYER
B SCHUSTER
R SUMMERS
RDRL WMM
J BEATTY
RDRL WMM B
G GAZONAS
D HOPKINS
B LOVE
B POWERS
RDRL WMM E
J SWAB
RDRL WMM F
T SANO
M TSCHOPP
RDRL WMM G
J ANDZELM
RDRL WMP
D LYON
J HOGGE
S SCHOENFELD
T VONG
RDRL WMP A
S BILYK
W UHLIG
J CAZAMIAS
P BERNING
J FLENIKEN
M COPPINGER
K MAHAN
C ADAMS
RDRL WMP B
C HOPPEL
M SCHEIDLER
T WEERASOORIYA
RDRL WMP C
S SATAPATHY
R BECKER
T BJERKE
D CASEM
J CLAYTON
M GREENFIELD
R LEAVY
J LLOYD
S SEGLETES
A SOKOLOW
A TONGE
C WILLIAMS

RDRL WMP D
A BARD
R DONEY
M KEELE
D KLEPONIS
C RANDOW
J RUNYEON
G VUNNI
M ZELLNER
RDRL WMP E
P SWOBODA
P BARTKOWSKI
D HORNBAKER
RDRL WMP F
C CUMMINS
D FOX
R GUPTA
RDRL WMP G
S KUKUCK
J STEWART